Computing Stable Contact Interface for Customized Surgical Jigs

Xiaoting Zhang[1], Ka-Chun Chan[1], Charlie C. L. Wang[1†], Kwok-Chuen Wong[2] and Shekhar-Madhukar Kumta[2]

Abstract— This paper presents a framework to compute stable contact interfaces for automatically designing customized jigs used in bone surgeries. Given the surface model of a bone represented by polygonal meshes, we find out a small region on the surface to be used as the interface of a customized jig so that it can be stably fixed on the bone under a directional clamping force. The variation of directions on the clamping force is allowed in our formulation. Moreover, the surface region serves as the interface of stable contact must also be disassemblable so that the jig and the bone can be separated after removing the clamping force. The analysis of stable contact is formulated on a Gaussian map by the common regions of half-spaces according to the motion restrictions. A flooding algorithm is proposed to determine those disassemblable and stable contact interfaces on the surface of a bone, where the contact surfaces are later converted into the solid model of a jig to be fabricated by additive manufacturing. Experimental tests are taken to verify the stable contact between a bone and the jig generated by our approach.

I. INTRODUCTION

With the advancement in 3D sensing technology, image-based navigation has become a widely accepted surgical technique for various *computer-assisted surgery* (CAS). CAS can be more safe and effective than the conventional treatment under appropriate usage and proper training. The general principles of CAS are not limited to the navigation during surgery. It can also be used in model generation, preoperative planning and surgical simulation before taking the actual surgery.

One important application of CAS for orthopaedic surgery is bone sarcoma surgery. The resection plan can be outlined preoperatively using CT/MRI images (see [1], [2]), by which position and orientation of a resection plane can be determined before hand. The precision of the resection plane is crucial since it should satisfy the oncological safe principle [3] to maximize the preservation of normal tissue and minimize the risk of recurrence caused by unclear tumor removal. It has been reported that with the help of computer navigation, the resection margins can be identified accurately at surgery [4]. However, the existing technique requires a bulk of navigation facilities (e.g., an optical camera, navigation trackers and instruments etc.) and the presence of a system operator in the operating room. Moreover, in practice,
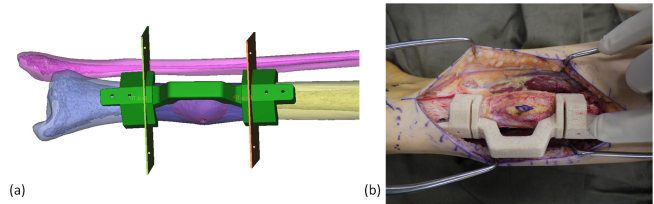
Fig. 1. With the help of customized jig in bone resection, the preoperatively planned resection path can be accurately performed during the operation: (a) specifying the customized jig integrated with planned paths and (b) using the jig fabricated by additive manufacturing in the bone tumor surgery.

the standard tools and techniques can substantially limit the ability to reliably and consistently reproduce the ideal preoperative plan at the time of resection [5]. For instance, it has been reported that an experienced surgeon might achieve a planned 1cm surgical margin ($\pm$ 5mm) with a probability of only 52% for a pelvic tumor resection surgery [6]. Integrating CAD planning into CAS allows complex tumor resections and the design of customized protheses for bone resection [7]. It has been reported that, with the help of this technique, the intralesional resection is reduced from 29% to 8.7% [8]. However, the design of customized CAD protheses requires engineers with substantial design experiences [5], which will usually take a week or more till the prothesis is ready for operation. As tumor may regression everyday, a more efficient technique is needed.

A. Motivation

The purpose of the research presented in this paper is to compact all the navigation facilities and the system operator into a customized jig, which can be landed on bones through touching the surface of the bone. Unique shape of the interface between bone and jig guarantees the accuracy of landing. With the help of such a customized jig, the coordinate systems of an imaging software and the physical environment can be precisely aligned.

In this paper, we investigate the technique to search a stable footprint on the surface of a bone for designing the customized jig. Specifically, from the scanned 3D model of a bone, we find a surface region as the touching interface to generate the customized jig, with which the motion between bone and jig is restricted under clamping forces. As a result, surgeons can easily place a customized jig at the right position and orientation on the bone, and the planned resection path integrated on the jig can be precisely realized during the bone resection (see Fig.1). The major challenge of this work comes from how to efficiently compute a
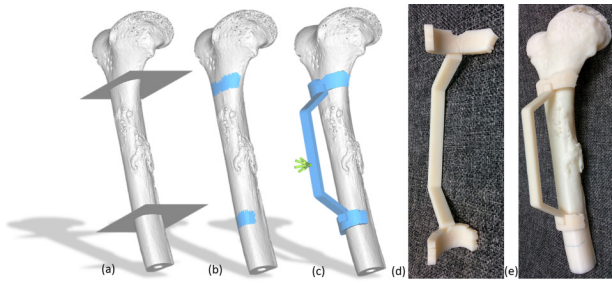
Fig. 2. Design automation of customized surgical jigs: (a) placing the resection paths with the reconstructed bone model, (b) computing the stable contact interface, (c) generating the solid for a customized jig, and (d) the jig fabricated by additive manufacturing.

region providing such a stable contact, using which as an interface must make the customized jig and the bone be disassemblable. We formulate the problem of stable contact by analyzing *configuration spaces* (C-space) on a Gaussian map and develop a flooding algorithm to determine the interface for stable contact.

The whole procedure for designing a customized jig can be completed automatically. As illustrated in Fig.2, for a bone model reconstructed from CT/MRI images, some planned resection paths are first specified in the imaging coordinate system (as Fig.2(a)). Seed regions can be obtained from the intersected triangles between the resection planes and the bone model. The unique interface for stable contact around the seed region can be determined by our flooding algorithm (see Fig.2(b)). The solid of a customized jig can be generated thereafter (see Fig.2(c)) and fabricated by *fused deposition modeling* (FDM) – a type of additive manufacturing (see Fig.2(d)).

B. Related Work

Patient specific instruments (PSI) such as customized jigs have been used to facilitate accurate resection and help to reproduce the preoperative plan reliably. Dental implant surgical guide has been widely used (ref. [9]). Other attempts on knee arthroplasty [10] and spinal instrumented surgery [11] have also been reported recently. Khan et al. [5] designed a patient specific jig to perform the bone tumor resection surgery with the help of two commercial CAD/CAM softwares. The contacting surface of a jig is designed to conform to the bone surface in the region surrounding the tumor, and three 3.2mm Steinmann pins are used to fix the jig while surgeons operating the saw cuts. Cartiaux et al. [12] performed a pelvic bone tumor surgery simulation to prove the accuracy of patient specific instrumentation technology. Again, pins are used to restrict the motion. Wong et al. [7] use additive manufacturing techniques to produce a surgical jig which has the corresponding anatomical shape of the bone surface that enables physical registration to the patient's anatomy. As a consequence, the jig can be positioned stably on the bone surface at the planned resection sites without using pins. However, neither conditions for a stable contact nor the method for determining the region of interface is

given. The concept of unique footprint is also employed in the work of Kunz et al. [13] to accurately and reliably perform femoral component placement. The interface of their jig consists of two parts: one for ensuring stable position and another for stopping rotation. In all these works, the method for automatically computing the unique footprint has not been investigated.

Some related work has been done in computer graphics for computing the unique registration between multiple pieces of components [14]. In their work, feature-based robust global registration has been taken to find out the matched interfaces between fractured components. Kinematic surface analysis has also been employed to process and recognize the geometry of mesh models in [15]–[17], which is based on computing the *degree-of-freedom* (DoF) of points' movement on the surface. However, kinematic surface analysis becomes not stable when the supporting size of interested region changes. Unfortunately, this is the case of interface search for customized jig – the area of a surface region to be analyzed are changed during the searching procedure. Moreover, it is hard to integrate the consideration of disassemblability into the framework of kinematic surface analysis.

Related to this proposed work, there are a lot of works on the fixture layout design in the literature where fixture is an important tool used to hold an object firmly for manufacturing [18], [19]. Brost and Goldberg [20] presented a complete algorithm for the fixture design problem of 2D polygonal parts by using three round locators and one translating clamp. The algorithm is later extended to 3D objects [21]. The contacts with fixture's locators and an object to be immobilized are usually point-based (e.g., [22], [23]), which is also the case in a similar robotic problem – grasping (ref. [24]). Differently, for a customized surgical jig with an interface conformal to the surface of a bone, the contacts are surface-based with more DoFs being constrained. This leads to the challenge of disassemblability in our problem. Moreover, the directional variation of clamping forces has not been considered in the prior works of fixture design.

Orientation-based motion analysis techniques have also been employed to solve a variety of manufacturing problems. Elber et al. [25] introduced a strategy for the 2-piece mold separability problem for a model whose surfaces are differentiable. The analysis is taken on a Gaussian map. Fogel and Halperin [26] presented an exact algorithm for solving the polyhedral assembly partitioning problem. They constructed the Minkowski sums of the convex subparts, and then analyzed the motion space on a Gaussian map. Suthunyatanakit et al. [27] proposed a geometric method to find the global accessibility of a polyhedral model. The analysis is also taken on the Gaussian map. As the boundaries of accessible regions needs to be explicitly stored in their method, the memory consumption becomes very expensive when a model with large number of faces is involved. Differently, in our framework, we only need to answer the questions of whether a C-space is empty. A simplified representation of C-space can be used here to compute the result effectively.

C. Contributions

The technical contributions of our work are:

- A formulation considering both immobilization and disassemblability of the contact between two objects with the freeform interface represented by polygonal mesh surfaces.
- A robust contact analysis and formulation based on the concept of θ-stable contact between two freeform objects.
- A computational scheme to determine a minimal stable contact surface between two freeform objects by the analysis taken on the Gaussian map.

To the best of our knowledge, this is the first approach to compute stable contacting interfaces of customized jigs for aligning the imaging and the physical coordinate systems in patient specific surgeries.

II. PROBLEM STATEMENT

Given the surface model of a bone represented by a triangular mesh $\mathcal{M} = \{t_i\}$, to find out a small region $\mathcal{B} \subset \mathcal{M}$ to use as the interface of a customized jig so that it can be stably placed on the bone after applying a directional clamping force $\mathbf{f}$.

To achieve the goal of computing a stable contact interface between a customized jig and a bone, a few factors need to be considered according to the usage of surgical jigs in the scenario of bone resection.

- **Stable Contact:** A jig must have a unique position and orientation when touching the surface of a bone by the computed interface. Once been landed and clamped, motions of the jig with reference to the bone are completely restricted. Such a property is also called form-closure. The form-closure must be stably retained even after allowing a perturbation on the direction of the clamping force $\mathbf{f}$. This will be formulated in Section III-B.
- **Disassemblability:** After releasing the clamping force, the jig and the bone should be able to separate. Specifically, the interface $\mathcal{B}$ must be disassemblable. This will be formulated in Section III-A.
- **Minimal Area:** To limit the expose area in surgery,
  $$\min \sum\nolimits_{t_j \in \mathcal{B}} A(t_j)$$
  is demanded where $A(\cdot)$ returns the area of a triangle. This is achieved by the flooding algorithm presented in Section IV-A.
- **Non-interference:** To keep tumor untouched during the resection, the interface cannot be overlapped with some restrictive regions specified during the surgery planning. This will also be realized by the flooding algorithm.

A region $\mathcal{B}$ on the surface of a bone is to be computed by incorporating all these factors. Formulation details are presented in the following section.

III. FORMULATION

For the polygonal mesh surface $\mathcal{B}$ on the bone, a co-incident mesh surface $\mathcal{B}'$ will be constructed on the jig

where every triangle in $\mathcal{B}'$ is duplicated from a corresponding triangle in $\mathcal{B}$ but with an inverse orientation. $\mathcal{B}$ and $\mathcal{B}'$ are overlapped with each other during the contact. Without loss of generality, when there are any two triangles $t_i, t_j \in \mathcal{B}$ ($i \neq j$) with $\mathbf{n}_i \times \mathbf{n}_j \neq 0$, the relative motion between $\mathcal{B}$ and $\mathcal{B}'$ can only be translational. Based on this reason, only translational motions applied on the jig need to be considered in our formulation. And norm of a motion vector $\mathbf{d}$ is less important in the analysis. As a consequence, our formulation is taken on a Gaussian map (i.e., $\mathbf{d} \in \mathbb{S}^2$).

A. Disassemblability

Unlike the conventional moldability evaluation conducted by 2D linear programming in a plane [28], the condition for the disassemblability of a polygonal mesh surface is formulated below on the Gaussian map to ease the formulation incorporating clamping forces.

Remark 1 For any planar triangle $t_i \in \mathcal{B}$, with normal vector $\mathbf{n}_i$, the translation of jig along a direction $\mathbf{d}$ has been *resisted* by the bone if $\mathbf{n}_i \cdot \mathbf{d} < 0$.

According to the constraint given in Remark 1, each $t_i \in \mathcal{B}$ forms a *disassemblable half-space* on $\mathbb{S}^2$ as

$$\mathcal{H}(t_i) = \{\mathbf{d} \in \mathbb{S}^2 \mid \mathbf{n}_i \cdot \mathbf{d} \geq 0\}. \tag{1}$$

For a region $\mathcal{B}$ consists of multiple triangles, its *disassemblable* C-space is defined as

$$\mathcal{C}_m(\mathcal{B}) = \bigcap_{t_i \in \mathcal{B}} \mathcal{H}(t_i). \tag{2}$$

Remark 2 A jig and a bone having the interface $\mathcal{B}$ is *disassemblable* if and only if $\mathcal{C}_m(\mathcal{B}) \neq \emptyset$.

B. Stable Contact

The movable C-space under *contact* and then the *stable contact* are formulated below.

Remark 3 For a jig contacting a bone at the region $\mathcal{B}$ under a clamping force $\mathbf{f}$, the movement of jig along a direction $\mathbf{d}$ is *resisted* if $\mathbf{f} \cdot \mathbf{d} < 0$.

The *movable* C-space according to $\mathbf{f}$ is then defined as a half-space:

$$\mathcal{H}_f = \{\mathbf{d} \in \mathbb{S}^2 \mid \mathbf{f} \cdot \mathbf{d} \geq 0\}. \tag{3}$$

The *movable* C-space of a jig under *contact* is defined as

$$\mathcal{C}_c(\mathcal{B}) = \mathcal{C}_m(\mathcal{B}) \bigcap \mathcal{H}_f \tag{4}$$

with $\mathcal{C}_m(\mathcal{B})$ being the *disassemblable* C-space of $\mathcal{B}$.

Remark 4 A contact between a jig and a bone with the interface $\mathcal{B}$ under a clamping force $\mathbf{f}$ is *fixed* if and only if $\mathcal{C}_c(\mathcal{B}) = \emptyset$.

Nevertheless, formulating a fixed contact as Remark 4 has the following difficulties in practice.

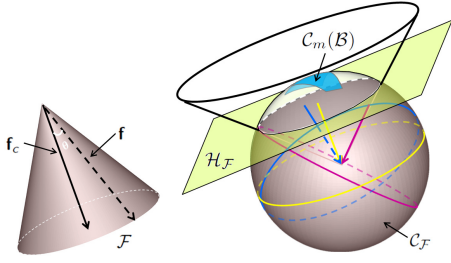- The direction of clamping force $\mathbf{f}$ is hard to be known by users.

Fig. 3. An illustration of a force-set, $\mathcal{F}$, and its corresponding movable C-space, $\mathcal{C}_{\mathcal{F}}$.

Fig. 4. Progressive results illustrating our flooding algorithm for computing the minimal stable contact interface.

- During the operations of bone resection, the direction of $\mathbf{f}$ can change.

To overcome these difficulties, stable contact is formulated as follows.

Definition 1 If the directional variation of $\mathbf{f}$ is within an angle θ with reference to a centrical direction $\mathbf{f}_c \in \mathbb{S}^2$, the set $\mathcal{F} = \{\mathbf{f} \in \mathbb{S}^2 \mid \mathbf{f}_c \cdot \mathbf{f} > \cos\theta\}$ is defined as the *force-set* for clamping.

Definition 2 The contact between a jig and a bone is called θ-*stable* if the contact is *fixed* under *all clamping forces* in the force-set.

By Definition 1 and Remark 3, we can have the movable C-space of force-set $\mathcal{F}$ on the Gaussian map as

$$\mathcal{C}_{\mathcal{F}} = \bigcup_{\mathbf{f}_k \in \mathcal{F}} \mathcal{H}_{\mathbf{f}_k} = \{\mathbf{d} \in \mathbb{S}^2 \mid \mathbf{f}_c \cdot \mathbf{d} + \sin\theta \geq 0\}, \quad (5)$$

which leads to the following remark for stable contact. Note that, $\mathcal{C}_{\mathcal{F}}$ defined above in Eq.(5) is coincident with the region defined by a planar half-space $\mathcal{H}_{\mathcal{F}}$ on $\mathbb{S}^2$. An illustration for the movable C-space of $\mathcal{F}$ is shown in Fig.3.

Definition 3 The *movable* C-space of a jig under any clamping forces in $\mathcal{F}$ is defined as

$$\mathcal{C}_{sc}(\mathcal{B}) = \mathcal{C}_m(\mathcal{B}) \bigcap \mathcal{C}_{\mathcal{F}} \quad (6)$$

Remark 5 The contact between a jig and a bone sharing the interface $\mathcal{B}$ is θ-*stable* if and only if $\mathcal{C}_{sc}(\mathcal{B}) = \emptyset$.

IV. COMPUTATION

This section presents the flooding algorithm to determine the minimal stable contact surface, the method to evaluate the feasibility of sets defined by half-spaces, and the method for converting a contact surface into the solid of a customized jig.

A. Flooding Algorithm

According to the design constraints analyzed in Section II, a flooding algorithm is developed to compute the minimal stable contact interface $\mathcal{B}$ by incrementally adding new triangles into $\mathcal{B}$. Here, a triangle t_b to be added into $\mathcal{B}$ is called an *disassemblable* triangle if $\mathcal{C}_m(\mathcal{B}) \bigcap \mathcal{H}(f_b) \neq \emptyset$ – i.e., adding it will not change the disassemblability of $\mathcal{B}$.
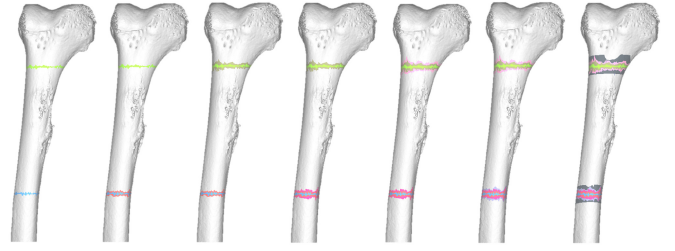
The algorithm starts from a seed region that is indicated by the surgery planners where the jig is going to land. The seed region is part of the bone's surface $\mathcal{M}$. A set of candidate triangles, $\mathcal{R}$, is first formed by the 1-ring neighbors of the current $\mathcal{B}$. Triangles are randomly selected from $\mathcal{R}$ to check if they can be added into $\mathcal{B}$. Only *disassemblable* triangles are added. Also, the triangles belonging to the restrictive regions (e.g., the places with tumor) must also be excluded. When $\mathcal{R}$ is empty, the algorithm rebuilds a new $\mathcal{R}$ by the current $\mathcal{B}$. After adding each triangle, the condition of θ-stable contact will be detected. By Remark 5, the iteration stops when $\mathcal{C}_{SC}(\mathcal{B}) = \emptyset$ (i.e., θ-stable contact has been achieved by $\mathcal{B}$).

Lastly, as a post-processing step of the interface searching, the bounding-box of $\mathcal{B}$ aligned with the axes from $\mathcal{B}$'s *principal component analysis* (PCA) is computed. The surface M is trimmed by this bounding-box, and the triangles inside the bounding-box are added into $\mathcal{B}$ if they are disassemblable. Note that this will not change the stableness of contact. As a result, the contact interface with relative regular boundary can be obtained.

B. Feasibility Computation

The flooding algorithm intensively uses the step of detecting whether the C-space commonly defined by a set of half-spaces on the Gaussian map is *empty*. We develop a simple and practical algorithm below for this purpose.

It is known from computational geometry [28] that the common region determined by a set of planar half-spaces is convex if there is a common region satisfying all the inequalities of the planar half-spaces – called *feasible* region. This idea is borrowed to our feasibility computation taken on the Gaussian map. We compute the corner points of the feasible convex region on the Gaussian sphere. The corner points of a C-space $\mathcal{C}_m(\mathcal{B})$ can be obtained by a search algorithm. For any two triangles t_i and t_j ($i \neq j$) in $\mathcal{B}$, two intersection points can be formed by their corresponding half-spaces on the Gaussian map. Among all these intersection points, only those are *feasible* for all half-spaces are kept in a list $\mathcal{Q}$ (i.e., satisfy the inequality of all half-spaces). Note that, as we assume that at least two triangles in $\mathcal{B}$ are not parallel to each other. For a C-space $\mathcal{C}_m(\mathcal{B}) \neq \emptyset$, $\mathcal{Q}$ must contain some corner points. The movable C-space $\mathcal{C}_{SC}(\mathcal{B})$ can also be detected in this way by using the planar half-space $\mathcal{H}_{\mathcal{F}}$ in the computation. Specifically, the condition of disassemblability

and θ-stable contact is detected as follows:

- The surface region $\mathcal{B}$ is disassemblable if the corner point set $\mathcal{Q}$ of $\mathcal{C}_m(\mathcal{B})$ is *not empty*.
- The surface region $\mathcal{B}$ achieves θ-stable contact when the set $\mathcal{Q}$ corresponding to $\mathcal{C}_{SC}(\mathcal{B})$ is *empty*.

Although the corner search algorithm has the theoretical complexity as $O(n^3)$, much better efficiency is observed in practice as many intersections can be quickly culled.

C. Solid Generation

After obtaining a stable contact interface $\mathcal{B}$, the solid model of a jig can be generated by first applying the thickening operator [29] to convert $\mathcal{B}$ into a solid $\mathcal{S}$ and then merging the accessory components with the help of Boolean operators [30] (see Fig.5). Note that, when converting $\mathcal{B}$ into $\mathcal{S}$, the following two criteria must be satisfied:

- **Exact:** To ensure a perfect match when placing the jig onto the surface of a bone, the portion of boundary surface on $\mathcal{S}$ according to $\mathcal{B}$ must be *exact* as $\mathcal{B}$ – i.e., without shape approximation error.
- **Interference-free:** The generated solid should not have interference with the bone model and should not go into the restrictive region with tumor presented.

In [29], a thicken solid $\mathcal{S}$ is defined in an implicit representation on one-side of $\mathcal{B}$ with the help of *signed distance-field* (SDF). The SDF can be efficiently evaluated in a narrow-banded region, and the isosurface of the implicit surface is partially extracted and stitched onto an inverse copy of $\mathcal{B}$. The exact is guaranteed. Moreover, the interference can be avoided by not allowing the implicit solid defined in the prohibited area. Also, the fast approximate Boolean operation introduced in [30] only changes meshes at the intersected regions so that the exact is also preserved in merging.
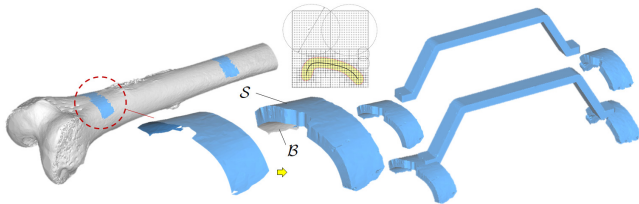
Fig. 5. The solid model of a jig can be generated by first applying the thickening operator, and then using the Boolean operators on the stable contact interface $\mathcal{B}$ and the other accessory components.

V. RESULTS AND VERIFICATION

A. Examples and Statistics

We have implemented the proposed algorithm in a proto-type system using C++ and OpenGL. Tests have been taken on a variety of bones. The customized jigs generated by our system are sent to a FDM 3D printing machine to fabricate the physical models.

In Fig.6, we demonstrate that different contact interface will be obtained when different values of θ are used in the computation. The larger θ is employed, a larger area of interface will be obtained. Although most surgical jigs in
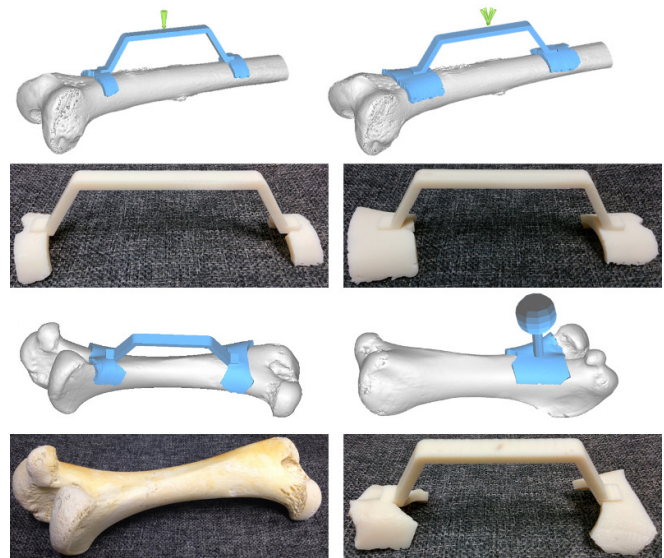
Fig. 6. Results of customized jigs generated by our prototype system – note that, when increasing the value of θ (changing from $25°$ and $35°$), a contact surface with larger area will be obtained. Here, the green arrows illustrate the range of clamping force-set.
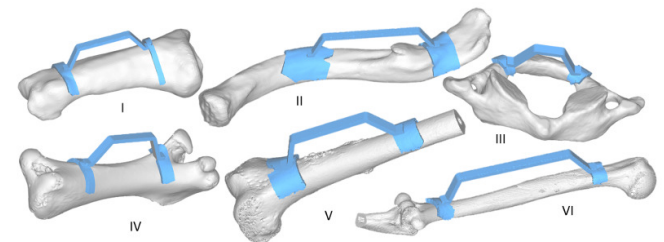
Fig. 7. More results with statistics on the number of triangles and the time for computation.

practice have two contact regions to achieve a stable landing after applying a clamping force, we also test the case with only one contact region. It is not surprised that a larger contact area is needed. The tests have been taken on more models of bones with a variety of shapes (see Fig.7). The θ-stable contact interface can be successfully computed in all the cases. The computational statistics are also given in Fig.7. It is easy to find that our approach can efficiently compute the stable contact interfaces on models with large number of triangles. For a bone model with more than 1.8 million triangles, the customized jig can be obtained in less than 12 seconds.

B. Physical Verification

Experimental tests are also taken to verify the physical performance of jigs generated by our approach. We build two setups for this purpose – one for translational loading and another for rotational loading (as illustrated in Fig.8). In the translational tests, a bone is fixed on a trolley which can slide along two inverse directions. A force sensor is connected to the trolley and reads *zero* when the trolley is in relax. When push and pull the trolley, the force sensor will response the received forces. In the rotational tests, a bone are fixed on a
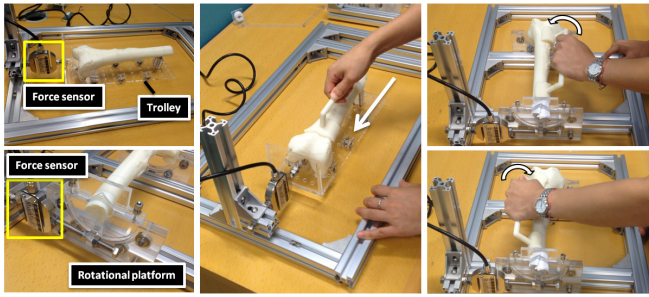
Fig. 8. The experimental setups for verifying the stable contact between the bone and a customized jig generated by our approach – both the translational loading and the rotational loading have been tested.

rotational platform which can rotate along the axis. A force sensor has one side linked to the rotational platform and another side fixed. When rotating the bone along the axis, the force sensor will response the received torques. The force sensor DYLY-102 with the accuracy 0.05% and the range up to $10kg$ is used in our verification.

In all tests, we land the jig at a random position and then slide it on the surface of bone while keep touching the bone. When users apply similar loadings (translational or rotational) on the handle of a jig at different contact places, different forces will be measured by the sensor:

- **Instable contact:** When instable contact is practiced, the relative motion between a jig and the bone is not completely restricted. The forces measured are mainly caused by frictions, which should be small.
- **Stable contact:** When a θ-stable is achieved, the jig and the bone are completely locked under a clamping force. In this scenario, whole loadings applied by the user can be measured by the sensor.

Our tests verify this as large forces can be measured when the jig is placed to a stable contacting place (see Fig.9). This occurs under both translational and rotational loadings.

To verify the contact surface generated by our method provides a stable-contact, another experiment is taken to measure the input/output loadings at the stable contacting place and other randomly picked places. In this experiment, two force sensors are used – one is attached onto the bone and another is locked with the jig. Two setups are built for both the translational and the rotational loadings (see Fig.10). The input and output loadings should be consistent when the jig and the bone are stably contacted. For other places, the forces measured on the output sensor are mainly caused by the friction, which are different from input. This phenomenon can be well observed from our tests (see Fig.11).

VI. CONCLUSIONS

In this paper, we present an approach to automatically design a customized jig for bone resection surgery. The technical contribution of our work is a geometric reasoning algorithm to determine a minimal surface area that provides stable contact between a jig and a bone. The stability of contact and the disassemblability has been formulated under a unique framework computed on the Gaussian map. The
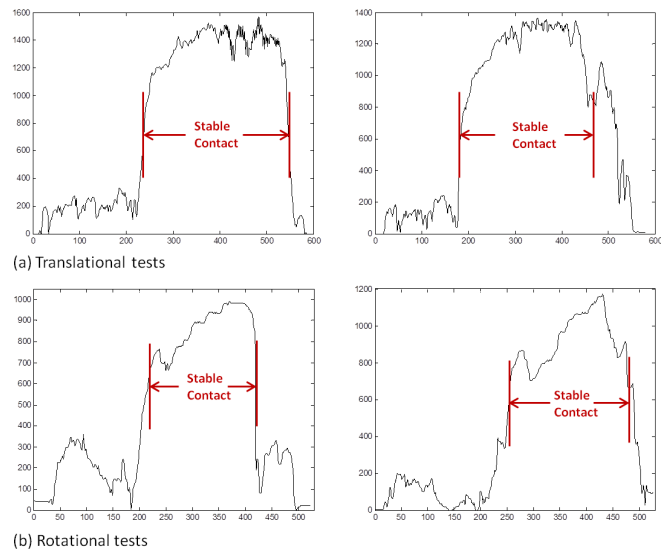

(a) Translational tests

(b) Rotational tests

Fig. 9. The measured forces under translational and rotational loadings when sliding a customized jig on the surface of a bone.
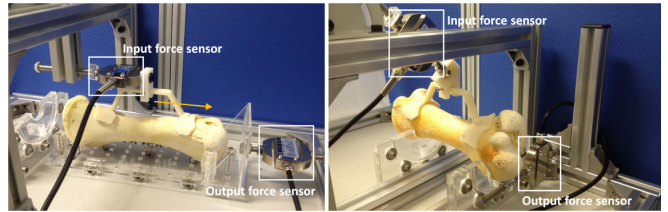

Fig. 10. The experimental setups for comparing the input/output loadings: (left) for translational loading and (right) for rotational loading.

results of our approach have been verified physically on the setups equipped with force sensors.

The results of our current approach is very encouraging. However, there are still some limitations to be overcome in the future work. First, the current computation relies heavily on the accuracy of the input bone model, and the shape approximation errors between the real bone and the imaged model have not been considered in our formulation. Although using a high-resolution imaging system can reduce the error, it will also lead to some safety issue caused by radiation. Second, as the FDM based additive manufacturing is employed to realize the customized jig physically, the fabricated jig may not completely retain the small features caused by the limited resolution of FDM. On the other hand, those small features contribute to the computation of stable contact. We also plan to realize a de-featuring technique on the surfaces of bones to remove those small features that cannot be fabricated.

REFERENCES

[1] K. C. Wong, S. M. Kumta, G. E. Antonio, and L. F. Tse, "Image fusion for computer-assisted bone tumor surgery," *Clinical orthopaedics and related research*, vol. 466, no. 10, pp. 2533–2541, 2008.
[2] K. C. Wong, S. M. Kumta, K. H. Chiu, G. E. Antonio, P. Unwin, and K. S. Leung, "Precision tumour resection and reconstruction using image-guided computer navigation," *Journal of Bone & Joint Surgery*, vol. 89, no. 7, pp. 943–947, 2007.

(a) Translational tests at stable contacting position

(b) Translational tests at random position

(c) Rotational tests at stable contacting position
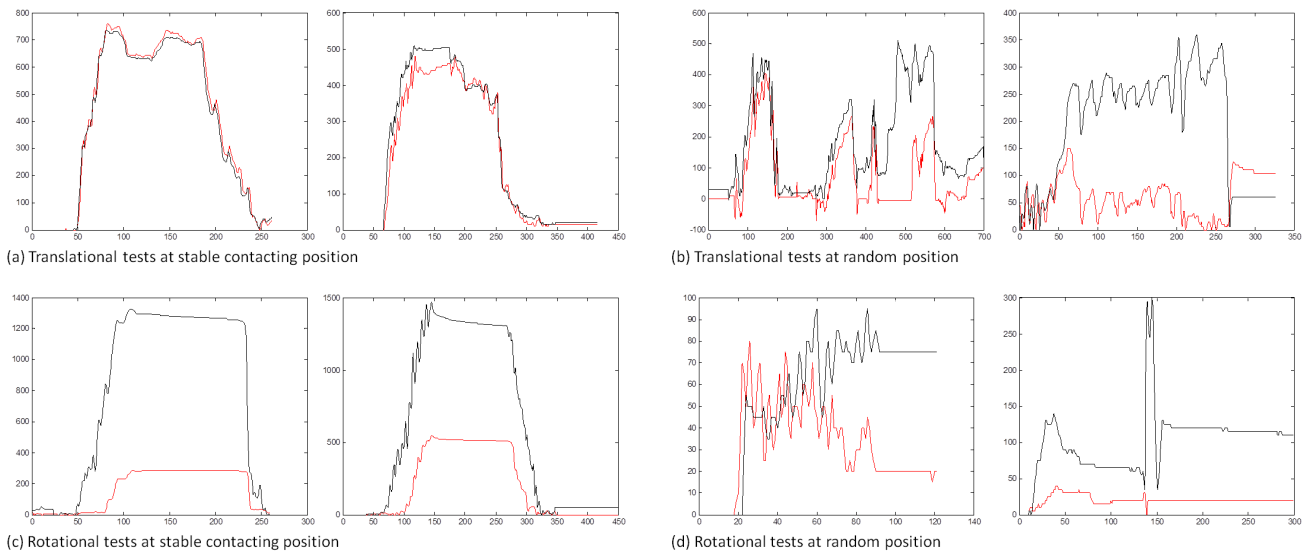
(d) Rotational tests at random position

Fig. 11. Input and output loadings measured at different places, where the input loadings are display in black curves and the output ones are in red. The measurement is taken at both the stable contacting place ((a) and (c)) and other random place ((b) and (d)). Loadings in two opposite directions are applied.

[3] D. S. Springfield, W. F. Enneking, J. R. Neff, and J. T. Makley, "Principles of tumor management," *Instructional course lectures*, vol. 33, pp. 1–25, 1983.

[4] K. C. Wong and S. M. Kumta, "Computer-assisted tumor surgery in malignant bone tumors," *Clinical Orthopaedics and Related Research*, vol. 471, no. 3, pp. 750–761, 2013.

[5] F. A. Khan, J. D. Lipman, A. D. Pearle, P. J. Boland, and J. H. Healey, "Surgical technique: Computer-generated custom jigs improve accuracy of wide resection of bone tumors," *Clinical Orthopaedics and Related Research*, vol. 471, no. 6, pp. 2007–2016, 2013.

[6] O. Cartiaux, P.-L. Docquier, L. Paul, B. G. Francq, O. H. Cornu, C. Delloye, B. Raucent, B. Dehez, and X. Banse, "Surgical inaccuracy of tumor resection and reconstruction within the pelvis: an experimental study," *Acta orthopaedica*, vol. 79, no. 5, pp. 695–702, 2008.

[7] K. C. Wong, S. M. Kumta, K. Y. Sze, and C. M. Wong, "Use of a patient-specific CAD/CAM surgical jig in extremity bone tumor resection and custom prosthetic reconstruction," *Computer Aided Surgery*, vol. 17, no. 6, pp. 284–293, 2012.

[8] L. Jeys, G. Matharu, R. Nandra, and R. Grimer, "Can computer navigation-assisted surgery reduce the risk of an intralesional margin and reduce the rate of local recurrence in patients with a tumour of the pelvis or sacrum?" *Bone & Joint Journal*, vol. 95, no. 10, pp. 1417–1424, 2013.

[9] C. M. Becker and D. A. Kaiser, "Surgical guide for dental implant placement," *The Journal of prosthetic dentistry*, vol. 83, no. 2, pp. 248–251, 2000.

[10] W. Fitz, "Unicompartmental knee arthroplasty with use of novel patient-specific resurfacing implants and personalized jigs," *The Journal of Bone & Joint Surgery*, vol. 91, pp. 69–76, 2009.

[11] S. Lu, Y. Q. Xu, W. W. Lu, G. X. Ni, Y. B. Li, J. H. Shi, D. P. Li, G. P. Chen, Y. B. Chen, and Y. Z. Zhang, "A novel patient-specific navigational template for cervical pedicle screw placement," *Spine*, vol. 34, no. 26, pp. E959–E966, 2009.

[12] O. Cartiaux, L. Paul, B. G. Francq, X. Banse, and P.-L. Docquier, "Improved accuracy with 3d planning and patient-specific instruments during simulated pelvic bone tumor surgery," *Annals of biomedical engineering*, vol. 42, no. 1, pp. 205–213, 2014.

[13] M. Kunz, J. F. Rudan, G. L. Xenoyannis, and R. E. Ellis, "Computer-assisted hip resurfacing using individualized drill templates," *Journal of arthroplasty*, vol. 25, no. 4, pp. 600–606, 2010.

[14] Q.-X. Huang, S. Flöry, N. Gelfand, M. Hofer, and H. Pottmann, "Reassembling fractured objects by geometric matching," *ACM Trans. Graph.*, vol. 25, no. 3, pp. 569–578, 2006.

[15] N. Gelfand and L. J. Guibas, "Shape segmentation using local slippage analysis," in *Proceedings of the 2004 Eurographics/ACM SIGGRAPH symposium on Geometry processing*, 2004, pp. 214–223.

[16] J. Andrews and C. Sequin, "Generalized, basis-independent kinematic surface fitting," *Computer-Aided Design*, vol. 45, no. 3, pp. 615–620, 2013.

[17] M. Bartoň, H. Pottmann, and J. Wallner, "Detection and reconstruction of freeform sweeps," *Computer Graphics Forum*, vol. 33, no. 2, pp. 23–32, 2014.

[18] Y. M. Rong, S. H. Huang, and Z. K. Hou, *Advanced computer-aided fixture design*. Academic Press, MA, USA, 2005.

[19] C. Wentink, A. F. van der Stappen, and M. Overmars, "Algorithms for fixture design," in *In J-P. Laumond and M.H. Overmars, editors, Algorithms for Robotic Motion and Manipulation*. A.K. Peters, 1996, pp. 321–346.

[20] R. Brost and K. Goldberg, "A complete algorithm for designing planar fixtures using modular components," *IEEE Trans. on Robotics and Automation*, vol. 12, no. 1, pp. 31–46, 1996.

[21] Y. Wu, Y. Rong, W. Ma, and S. LeClair, "Automated modular fixture planning: Geometric analysis," *Robotics and Computer-Integrated Manufacturing*, vol. 14, no. 1, pp. 1–15, 1998.

[22] Y. Zheng, M. C. Lin, and D. Manocha, "Efficient simplex computation for fixture layout design," *Comput. Aided Des.*, vol. 43, no. 10, pp. 1307–1318, 2011.

[23] M. Wang and D. Pelinescu, "Optimizing fixture layout in a point-set domain," *Robotics and Automation, IEEE Transactions on*, vol. 17, no. 3, pp. 312–323, 2001.

[24] Y.-H. Liu, M. ling Lam, and D. Ding, "A complete and efficient algorithm for searching 3-d form-closure grasps in the discrete domain," *IEEE Trans. on Robotics*, vol. 20, no. 5, pp. 805–816, 2004.

[25] G. Elber, X. Chen, and E. Cohen, "Mold accessibility via gauss map analysis," *Journal of Computing and Information Science in Engineering*, vol. 5, no. 2, pp. 79–85, 2005.

[26] E. Fogel and D. Halperin, "Polyhedral assembly partitioning with infinite translations or the importance of being exact," *IEEE Trans. on Auto. Sci. and Eng.*, vol. 10, no. 2, pp. 227–241, 2013.

[27] K. Suthunyatanakit, E. L. J. Bohez, and K. Annanon, "A new global accessibility algorithm for a polyhedral model with convex polygonal facets," *Computer-Aided Design*, vol. 41, no. 12, pp. 1020–1033, 2009.

[28] M. deBerg, O. Cheong, M. v. Kreveld, and M. Overmars, *Computational Geometry: Algorithms and Applications*, 3rd ed., 2008.

[29] C. C. L. Wang and Y. Chen, "Thickening freeform surfaces for solid fabrication," *Rapid Prototyping J.*, vol. 19, no. 6, pp. 395–406, 2013.

[30] C. C. L. Wang, "Approximate boolean operations on large polyhedral solids with partial mesh reconstruction," *IEEE Trans. on Vis. and Comp. Graph.*, vol. 17, no. 6, pp. 836–849, 2011.